ELSEVIER

Journal of Power Sources 54 (1995) 393–396

JOURNAL OF POWER SOURCES

Electro-thermal modelling of polymer lithium batteries for starting period and pulse power

P. Baudry [a], M. Neri [a], M. Gueguen [b], G. Lonchampt [c]

[a] *Electricité de France DER, Site des Renardières, Morêt-sur-Loing, France*
[b] *Bolloré Technologies, Odet, BP 607, 29551 Quimper Cedex, France*
[c] *CEA/CEREM, CENG-85X, 38041 Grenoble, France*

Abstract

Since power capabilities of solid polymer lithium batteries can only be delivered above 60 °C, the thermal management in electric-vehicle applications has to be carefully considered. Electro-thermal modelling of a thermally insulated 200 kg battery was performed, and electrochemical data were obtained from laboratory cell impedance measurements at 20 and 80 °C. Starting at 20 °C as initial working temperature, the battery reaches 40 °C after 150 s of discharge in a 0.5 Ω resistance. At 40 °C, the useful peak power is 20 kW. The energy expense for heating the battery from 20 to 40 °C is 1.4 kWh, corresponding to 6% of the energy available in the battery. After a stand-by period of 24 h, the temperature decreases from 80 to 50 °C, allowing efficient starting conditions.

Keywords: Lithium batteries; Polymer electrolyte cells; Thermal modelling

1. Introduction

Thin-film polymer electrolyte lithium batteries have received much attention during the last ten years [1–4] and large developments are in progress worldwide, especially in the application of electric vehicles. The large energy density provided by the lithium anode combined with an all-solid-state configuration, giving safety and durability and allowing automated manufacturing processes, are the main advantages suggested. However, diffusion kinetics in the polymer electrolyte and charge-transfer resistances at the lithium/electrolyte and cathode/electrolyte interfaces at low temperature limit the battery power density. Since the temperature dependence of the impedances is high, thermal management in large-scale batteries has to be carefully considered and the working temperature will be in the 50–100 °C range.

Modelling of lithium batteries (liquid or polymer electrolytes) has been reported by several groups. West and co-workers have studied the dynamics of the composite insertion electrode, taking into account, in a first time, the salt concentration gradient of the electrolyte contained in the cathode [5], and in a second time, the charge transfer and Li^+ diffusion in the insertion material [6]. More recently, Doyle et al. [7] used the concentrated solution theory in their simulation of the electrolyte phase. Lithium, polymer electrolyte and composite cathode electrochemical phenomena were all included in this general model.

Munshi and Owens [8] investigated the influence of the polymer battery configuration on their performance like energy density, pulse power density and sustained power density. They assumed that the internal battery resistance was governed by the electrolyte resistance.

Finally, results of the thermal behaviour of a 400 kg lithium polymer battery, proposed for an electric-van traction, were given by Kapfer et al. [9]. The heat loss and the total energy efficiency for this configuration were assessed but the dynamic behaviour was not described.

Following the previous works mentioned above, this paper describes in a first approach an electro-thermal modelling of a 200 kg lithium polymer battery. The main objective is to give some information on the available power and its thermal behaviour during starting and resting periods.

SSDI 0378-7753(94)02109-G

2. Model assumptions

2.1. Electrochemical data

A macroscopic approach is considered for this model. The electrical parameters used result from the electrochemical battery behaviour, investigated on laboratory cells by impedance spectroscopy. The Randles equivalent circuit shown in Fig. 1 has been proposed to describe the lithium battery response to an alternative voltage. R_{el} is the ohmic resistance of the electrolyte and current collector, C_{dl} is the double-layer capacitance at the cathode/electrolyte and lithium/electrolyte interfaces, R_{ct} is the charge-transfer resistance, and Z_w is a complex impedance arising from the diffusion of Li^+, often known as the Warburg impedance. When the impedance spectroscopy technique is used in the frequence range from 10^5 to 10^{-2} Hz, R_{el}, R_{ct} and Z_w can be obtained from the complex impedance representation as shown in Fig. 2.

In order to obtain these parameters experimentally, laboratory lithium polymer batteries were set up. The polymer electrolyte was a complex of modified poly(ethylene oxide) (PEO) and a lithium salt. The cathodic material was a commercial grade V_2O_5. Both polymer electrolyte and composite cathode (V_2O_5+PEO+C) films were prepared by the solvent-casting method and hot-pressed with a lithium anode after drying in a glove box. The cell active area was 7 cm^2. Electrolyte and cathode thickness were respectively 150 and 80 μm.

Impedance plots on the complex plane of such a lithium polymer cell at 20 and 80 °C are shown in Fig. 3. R_{el} and R_{ct} were obtained from these results according to the Randles equivalent circuit mentioned before. The temperature dependence was described with an Arrhenius behaviour. The problem of the diffusion limitation occurring after a few minutes of discharge

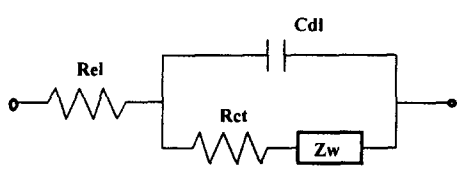

Fig. 1. Randles equivalent circuit of the lithium polymer battery: R_{el} = ohmic resistance; C_{dl} = double-layer capacitance; R_{ct} = charge-transfer resistance, and Z_w = Warburg impedance.

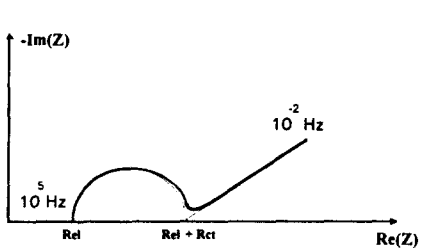

Fig. 2. Complex response of the Randles equivalent circuit with impedance spectroscopy.

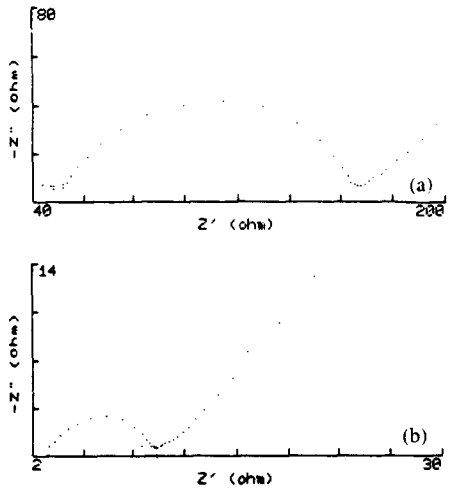

Fig. 3. Impedance plot of a 7 cm^2 lithium polymer battery in the 10^5–10^{-2} Hz range: (a) at 20 °C, and (b) at 80 °C.

and represented on the impedance plot at low frequencies is more difficult to assess. As the purpose of this work is not to give a simulation of the full discharge but only during the first minutes, we considered that the diffusional resistance (R_{diff}) was described by the following equation:

$$R_{diff} = R^0_{diff} t^{1/2} 10^{(B/T)} \quad (1)$$

where t is the time of discharge, T the temperature, and B a constant calculated from the experimental data.

Then, the global internal resistance (R) of the battery is given by:

$$R = R_{el} + R_{ct} + R_{diff} \quad (2)$$

The electronic current collector resistance is not considered, nor the increase in the electrochemical internal resistance versus cycling. This should be introduced in the next step of the modelling when experimental data, after cycling, are available.

2.2. Battery configuration

The single-cell weight is 2 kg with an energy density of 120 Wh/kg. The voltage used for the power calculation is 2.5 V, corresponding to 50% depth-of-discharge. The film thicknesses considered for the model are: 80 μm for the cathode (60 wt.% V_2O_5, 33 wt.% polymere, 7 wt.% C), 50 μm for the electrolyte, 30 μm for the lithium, 5 μm for the cathode nickel collector, and 5 μm for a polypropylene layer. This gives rise to an electrochemical surface are of 6.0 m^2, with an average cell gravimetric density of 2 g/cm^3. The battery is obtained by stacking 100 of these elementary cells in series. Therefore, the stored energy is 24 kWh with a mid-discharge voltage U of 250 V. The electrochemical parameters extrapolated from experimental laboratory cells to this configuration are shown in Table 1.

Table 1
Electrochemical parameters adopted for the model

Symbol	Parameter	Model assumption
σ(S/cm)	Electrolyte conductivity	2×10^{-5} at 20 °C 5×10^{-4} at 80 °C
R_{ct}(Ω cm^2)	Total charge-transfer resistance	800 at 20 °C 40 at 80 °C
R^0_{diff}(Ω cm^2/s^2)	Diffusional resistance constant	50 at 20 °C 10 at 80 °C
U(V)	Mid-charge battery voltage	250
R(Ω)	Total electrical battery resistance	$1.8+8.5\times10^{-2}t^{1/2}$ at 20 °C $0.085+1.7\times10^{-2}t^{1/2}$ at 80 °C

Table 2
Heat capacities of the single cell materials

Material	Heat capacity (J/(kg K))	Weight content in the battery (wt.%)
V_2O_5	700	34.0
Nickel	420	13.6
Polymer electrolyte	1460	41.6
Lithium	3500	5.3
Polypropylene	1500	1.5
Graphite	690	4.0

During the warming up, the thermal energy is delivered by the battery itself, discharging at a constant 0.5 Ω resistance (Z) located within the insulation case.

2.3. Thermal data

The heat capacity and mass proportions of the different materials included in the battery are listed in Table 2. The average heat capacity C_p is 1340 J (kg K).

The thermal insulation considered is 5 cm thick (l_1) with a thermal conductivity (λ_1) of 0.015 W (m K). As the battery volume is 100 l, this insulated case is 1 m long, 0.5 m large and 0.2 m high, giving rise to a 1.6 m^2 surface area (S_1). Heat runaway is assumed to occur across the insulation case and by external copper collectors, which are 0.1 m long (l_2) with a thermal conductivity λ_2 of 700 W (m K), and which have a cross section of 100 mm ^{2} (S_2), allowing a current intensity of 500 A. Internal cooling system, including a heat exchanger and a cooling vent are not provided in this model.

3. Results

The temperature evolution is obtained from the thermal equation:

$$U^2/(R+Z)-\lambda_1 S_1(T-T_{ext})/l_1-\lambda_2 S_2(T-T_{ext})/l_2 = Mc_p\,dT/dt \quad (3)$$

where T is the battery temperature, T_{ext} the external temperature and M the battery weight.

The battery temperature during the warming up is shown in Fig. 4. The temperature of 40 °C is obtained after 150 s for an initial battery temperature of 20 °C. The constant T_{ext} is 10 °C.

The evolution of the maximal useful power ($U^2/4R$) is shown in Fig. 5, with a temperature fixed at 80 and 40 °C. At the beginning of the discharge, the power reaches 120 kW at 80 °C, corresponding to a pulse power density of 600 W/kg. It still is 20 kW at 40 °C, high enough for an electric-vehicule starting. According

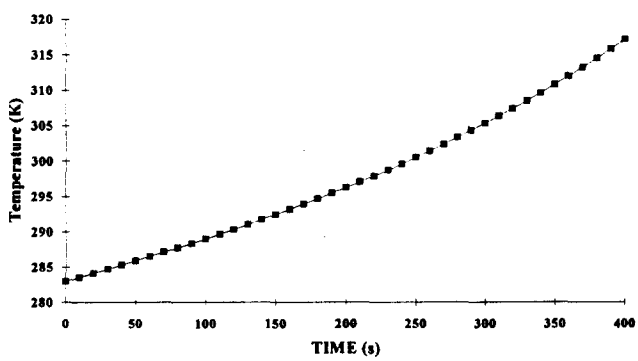

Fig. 4. Battery temperature evolution during warming up; external temperature is 10 °C.

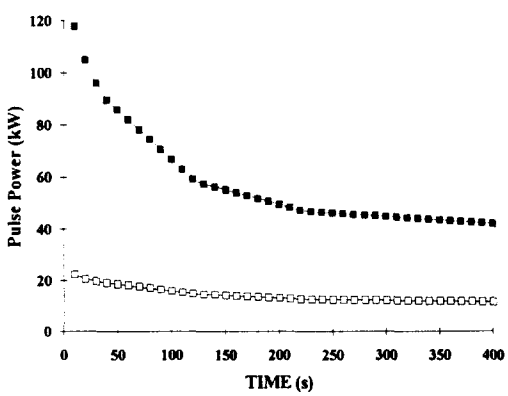

Fig. 5. Available battery pulse power at fixed temperature: (-■-) at 80 °C, and (-□-) at 40 °C.

to this fixed temperature condition, the power decreases while discharging, but remains reasonable during the 300 first seconds.

The energy expense for heating the vehicle during the warming up is presented in Fig. 6. For a 20 °C temperature increase, 1.4 kWh are expended, i.e. 6% of the energy available in the battery. This is in good agreement with the results obtained by Kapfer et al. [9].

In Fig. 7, the evolution of thermal losses, due to the insulation case and external collectors, shows that maintaining the temperature of 40 °C, with an outside temperature of 10 °C, would require 60 W, i.e. 1.4 kWh for 24 h, representing 6% of the stored energy. Inversely, it can be observed on the cooling curve of Fig. 8 that, out of operation, the temperature would decrease from 80 to 50 °C after 24 h, allowing efficient starting conditions.

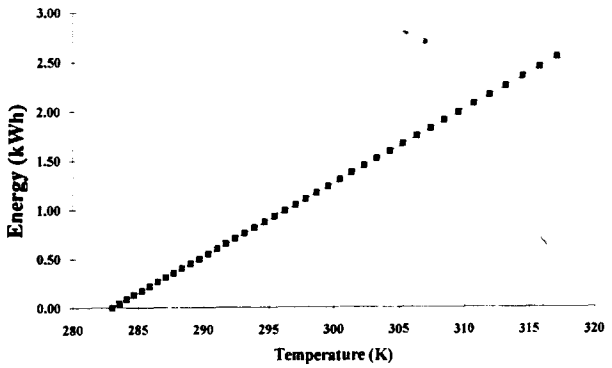

Fig. 6. Energy expense for the battery heating.

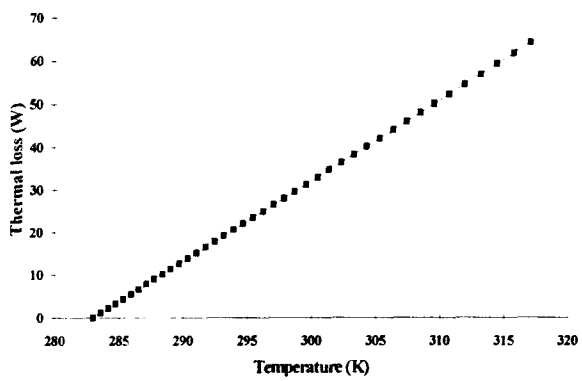

Fig. 7. Thermal loss vs. battery temperature; external temperature is 10 °C.

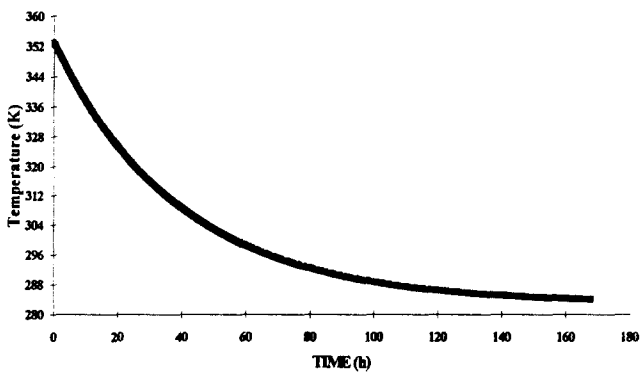

Fig. 8. Battery cooling vs. time; external temperature of 10 °C.

During normal discharging conditions between 60 and 80 °C, the thermal management must allow the battery to be cooled, while thermal losses will be lower than the thermal power dissipated by the battery. For a 10 kW useful battery power, under the electrochemical model assumptions, the battery thermal losses will be near 100 W, easy to remove with an appropriate cooling system.

4. Conclusions

Although this work does not pretend describing the actual lithium polymer battery behaviour during the full discharge, it suggests that their electrochemical characteristics, related to the thermal battery environment, can fullfill the electric-vehicle requirements, regarding the thermal-management problem. Warming up could possibly be boosted with an auxiliary power source if the external temperature is too low. Further improvements of this model need to be assessed, such as power decrease with cycling, temperature gradient within the battery case and optimization of electrochemical assumptions. Particularly, actual diffusion limitations after several minutes of discharge should be evaluated more accurately.

References

[1] M. Armand, J.M. Chabagno and M. Duclot, in P. Vashita (ed.), *Fast Ion Transport in Solids*, North-Holland, Amsterdam, 1979, p. 131.

[2] J.S. Lundsgaard, S. Yde-Andersen, R. Koksbang, D.R. Shackle, R.A. Austin and D. Fauteux, in B. Scrosati (ed.), *Proc. 2nd Int. Symp. on Polymer Electrolytes*, Elsevier Applied Science, Barking, UK, 1989, p. 395.

[3] M. Gauthier, D. Fauteux, G. Vassort, A. Belanger, M. Duval, P. Ricoux, J.M. Chabagno, D. Muller, P. Rigaud, M.B. Armand and D. Deroo, *J. Electrochem. Soc., 132* (1985) 1333–1340.

[4] R.J. Neat, W.J. Macklin and R.J. Powel, in B. Scrosati (ed.), *Proc. 2nd. Int. Symp. on Polymer Electrolytes*, Elsevier Applied Science, Barking, UK, 1989, p. 421–431.

[5] K. West, T. Jacobsen and S. Atlung, *J. Electrochem. Soc., 129* (1982) 1480–1485.

[6] B.C. Knutz, K. West, B. Zachau-Christiansen and S. Atlung, *J. Power Sources, 43/44* (1993) 733–741.

[7] M. Doyle, T.F. Fuller and J. Newman, *J. Electrochem. Soc., 140* (1993) 1526–1533.

[8] M.Z.A. Munshi and B.B. Owens, *Solid State Ionics, 38* (1990) 87–107.

[9] B. Kapfer, M. Gauthier and A. Belanger, in K.M. Abraham and M. Salomon (eds.), *Proc. Symp. Primary and Secondary Batteries*, 1991, pp. 227–234.